

Fort Hays State University

FHSU Scholars Repository

Master's Theses

Spring 2020

An assessment of convergence in the feeding morphology of *Xiphactinus audax* and *Megalops atlanticus* using landmark-based geometric morphometrics

Edward Chase Shelburne

Fort Hays State University, edward.c.shelburne@gmail.com

Follow this and additional works at: <https://scholars.fhsu.edu/theses>



Part of the [Biostatistics Commons](#), [Evolution Commons](#), [Multivariate Analysis Commons](#), [Other Animal Sciences Commons](#), [Paleobiology Commons](#), [Paleontology Commons](#), [Structural Biology Commons](#), and the [Zoology Commons](#)

Recommended Citation

Shelburne, Edward Chase, "An assessment of convergence in the feeding morphology of *Xiphactinus audax* and *Megalops atlanticus* using landmark-based geometric morphometrics" (2020). *Master's Theses*. 3151.

DOI: 10.58809/FBRA1021

Available at: <https://scholars.fhsu.edu/theses/3151>

This Thesis is brought to you for free and open access by FHSU Scholars Repository. It has been accepted for inclusion in Master's Theses by an authorized administrator of FHSU Scholars Repository. For more information, please contact ScholarsRepository@fhsu.edu.


AN ASSESSMENT OF CONVERGENCE IN THE FEEDING MORPHOLOGY OF
XIPHACTINUS AUDAX AND *MEGALOPS ATLANTICUS* USING
LANDMARK-BASED GEOMETRIC MORPHOMETRICS

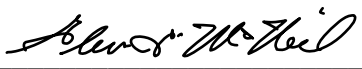
A Thesis Presented to the Graduate Faculty
of the Fort Hays State University in
Partial Fulfillment of the Requirements for
the Degree of Master of Science

by

Edward Chase Holt Shelburne
B.S., Texas State University

Date _____

Approved 
Major Professor

Approved 
Chair, Graduate Council

GRADUATE COMMITTEE APPROVAL

The graduate committee of Edward C. H. Shelburne approves this thesis as meeting partial fulfillment of the requirements for the Degree of Master of Science.

Approved Lawrence Wil

Approved John Chamell

Approved Reese E. Bennett

Date _____

ABSTRACT

Convergence is an evolutionary phenomenon wherein distantly related organisms independently develop features or functional adaptations to overcome similar environmental constraints. Historically, convergence among organisms has been speculated or asserted with little rigorous or quantitative investigation. More recent advancements in systematics has allowed for the detection and study of convergence in a phylogenetic context, but this does little to elucidate convergent anatomical features in extinct taxa with poorly understood evolutionary histories. The purpose of this study is to investigate one potentially convergent system—the feeding structure of *Xiphactinus audax* (Teleostei: Ichthyodectiformes) and *Megalops atlanticus* (Teleostei: Elopiformes)—using a comparative anatomical approach to assess the degree of shared morphospace occupation. *X. audax* was a large, predatory fish that inhabited the Western Interior Seaway (WIS) during the Late Cretaceous and went extinct 66 mya. *M. atlanticus*—the Atlantic tarpon—is a large elopiform fish that inhabits the Gulf and Atlantic coasts. Because of structural similarities in their crania and post-crania, *M. atlanticus* is often used formally and informally as a modern analog for *X. audax*.

Landmark-based geometric morphometrics (GM) was applied to determine the structural similarity in the feeding morphology of these two fish species. Six *X. audax* and six *M. atlanticus* specimens were 3D scanned and reconstructed as 3D models, and the GM procedure was conducted on in both 2D and 3D treatments. Principal components analysis (PCA), discriminant function analysis (DFA), sequential agglomerative hierarchical non-overlapping (SAHN) cluster analysis, and a multi-

response permutation procedure (MRPP) were all performed to quantify the shape difference between the 12 specimens.

All analyses produce comparable results. *X. audax* and *M. atlanticus* differ significantly in the structure of their feeding morphology and do not overlap considerably in morphospace, casting doubt on the idea that *X. audax* and *M. atlanticus* are structurally convergent in their feeding morphology. Most notably, there are substantial differences in the size and shape of the premaxilla, the length of the maxilla, and the inflection of the anterior dentary. The differences in these structures likely relate to the preferred feeding habits of each fish, with *X. audax* preferring large individual prey, and *M. atlanticus* relying on suction feeding to consume smaller schooling prey. These results suggest *M. atlanticus* is a poor modern analog for *X. audax* with respect to feeding morphology.

ACKNOWLEDGEMENTS

I would like to thank my and acknowledge my late mother Trevalyn Sabrina Holt for all of the time she spent reinforcing my love of nature and science throughout my formative years. I also want to thank my father, Dave Shelburne, for continuing to raise and support me and my brother Hunter and ensuring I received the skills and education to make it this far in life. My grandfather Charles Edward Holt has also been a pillar throughout my early life and academic ventures. The love and support of these family members, and many more, are the backbone of my success thus far, and they cannot be overstated.

I would also like to thank my many friends and support network that have kept me sane and helped me weather many a mental storm throughout my undergraduate and graduate career. Josh Martinez, Julian Moreno, Olivia Fruia, Kat Rivers, Rachel Unruh, Amber Michels, and many, many others have been invaluable in every aspect of my life and mental health. I must also extend a special and heartfelt acknowledgement to the late Dr. Ann Molineux, my friend and mentor during my five years at the University of Texas. Her kindness, cheer, and unconditional support are almost single-handedly responsible for my admission into graduate school and any success I sustain is directly attributable to her.

Next, I would like to thank my committee members. Dr. Laura Wilson, my adviser, for all of her support, advice, understanding, and provision of opportunity. Dr. Rob Channell for his never-ending expertise in life science and statistics that I can only hope to one day achieve. Dr. Reese Barrick for being Reese and for not firing me. Collectively I would like to thank them for editing this document and providing

constructive criticisms and critiques that have improved my abilities as a scientist and researcher.

Finally, I must acknowledge all of the museum faculty and staff around the country who assisted me in bringing this project to fruition by allowing me access to their fossil and osteological collections, as well as the Western Interior Paleontological Society (WIPS) and the Geological Society of America (GSA) which provided funding for travel to these institutions. This includes faculty and staff at the American Museum of Natural History, the Smithsonian National Museum of Natural History, the Florida Museum of Natural History, the North Carolina Museum of Natural Sciences, The University of Texas Biodiversity Center, and Fort Hays State University's Sternberg Museum of Natural History for providing specimens for this study. I also want to give a very special thank you to Hannah Horinek who helped me digitize several specimens used in this study.

TABLE OF CONTENTS

ABSTRACT.....	iii
ACKNOWLEDGEMENTS.....	v
TABLE OF CONTENTS.....	vii
LIST OF TABLES.....	ix
LIST OF FIGURES.....	x
INTRODUCTION.....	1
MATERIALS AND METHODS.....	8
Institutional Abbreviations.....	8
Materials.....	8
Data Collection.....	10
<i>Specimen</i> Digitization.....	10
<i>Specimen</i> Reconstruction.....	11
Data Analysis.....	14
<i>Landmark</i> Placement.....	15
<i>General Procrustes Superimposition and Principal Components</i> <i>Analysis</i>	16
<i>Discriminant Function Analysis</i>	17
<i>SAHN Clustering Analysis</i>	18

<i>Multi-response Permutation Procedure</i>	19
RESULTS.....	21
<i>Outlier Analysis</i>	21
<i>Principal Components Analysis</i>	21
<i>Discriminant Function Analysis</i>	25
<i>SAHN Clustering Analysis</i>	25
<i>Multi-response Permutation Procedure</i>	26
DISCUSSION.....	28
CONCLUSIONS.....	36
LITERATURE CITED.....	39
TABLES AND FIGURES.....	49

LIST OF TABLES

Table

1	Study specimens and their standard length.....	49
2	MRPP analysis values.....	49
3	Explanatory values of the first four PC axes.....	50

LIST OF FIGURES

Figure

1	Jaw angle, gape size, and gape width schematic.....	51
2	Example landmark placement.....	52
3	PCA 2D results.....	53
4	PCA 3D unadjusted results.....	54
5	PCA 3D outlier-adjusted results.....	55
6	DFA results.....	56
7	SAHN cluster results.....	57

INTRODUCTION

Convergence is an evolutionary phenomenon wherein two or more organisms evolve some similarity independently rather than through shared ancestry (Arbuckle & Speed, 2016), though other authors have defined convergence in different ways with differing levels of specificity (e.g. Stayton, 2015; Ingram & Mahler, 2008; Leander, 2009; Leander, 2008; Doolittle, 1994; Moore & Willmer, 1997). There are many different forms of convergence, including structural convergence (shared morphology), functional convergence (shared functional anatomy), developmental convergence (shared ontogeny), and sequence convergence (shared amino acid sequences) (Moore & Willmer, 1997; Doolittle, 1994; Wray, 2002). Numerous systematic approaches have been generated to detect the presence and strength of convergence in a phylogeny (Arbuckle & Speed, 2016, Speed & Arbuckle, 2016; Stayton, 2015; Arbuckle et al., 2014; Mahler et al., 2013; Stayton, 2006). However, because structure is the only observable form of convergence in the fossil record, developing methods for directly quantifying allegedly shared structure between unrelated organisms also has implications for understanding the function of these structures and the life history of the organisms. If the potentially convergent structure cannot be quantified in a comparative anatomical context, inferences regarding the function of these structures cannot be reliably inferred.

The purpose of this study is to examine one such potentially convergent system—the structurally similar feeding morphology of *Xiphactinus audax* Leidy 1870 and *Megalops atlanticus* Valenciennes 1846—using landmark-based geometric morphometric (GM) analysis to assess claims of convergence by investigating morphospace occupation.

If no significant shape difference is found between the feeding morphology of *X. audax* and *M. atlanticus*, then it is suggestive that these fish exhibit structural homoplasy in their feeding morphology (i.e. convergence or parallelism). While shared ancestry could also account for such similarity, qualitative assessment of the feeding structure of non-megalopid elopomorphs indicate a derived feeding condition for *Megalops* (discussed below). Findings of significant shape difference between the species' feeding morphology do not necessarily refute a homoplastic explanation, as convergence may still occur among taxa without morphospace overlap. However, comparing morphospace occupation is still a critical component of testing any potentially convergent system. Landmark based GM is a series of statistical techniques that quantify the shape of a set of objects while retaining the geometric data throughout the analysis—data which are typically lost in 'traditional' or linear morphometric techniques (Souter et al., 2010; Slice, 2007; Adams et al., 2004; Parsons et al., 2003; Rohlf & Marcus, 1993). A presupposition for employing this technique is that for a particular structure or structural suite to be considered structurally convergent, they should show a high degree of morphological similarity (i.e. similarity in shape) and therefore overlap in morphospace. Landmark-based GM has been used to investigate evolutionary divergence among continuous populations of fish, amphibians, and mammals (Cureton II & Broughton, 2016; Deitloff et al., 2016; Skoglund et al., 2015; Sakamoto & Ruta, 2012; Adams, 2010; Siwertsson et al., 2010; Langerhans et al., 2003), and another study by Piras et al. (2010) used traditional GM techniques to assess convergence between *Gavialis* (gharial) and *Tomistoma* (false gharial). Only one study has utilized landmark-based GM to assess convergence in a manner similar to the work presented here (Muschick et al., 2012) and

no prior studies have employed landmark-based GM techniques to investigate convergence in fossil organisms.

Xiphactinus is an extinct genus of ichthyodectiform fish from the Late Cretaceous, with a cosmopolitan distribution ranging from North America to Europe to Australia (Schwimmer, 1997; Bardack, 1965). In North America, fossils are known primarily from Cenomanian through Campanian outcrops of the Western Interior Seaway (WIS), an epicontinental sea that intermittently ranged from the arctic to the modern-day Gulf of Mexico (Murray & Cook; 2016; Vavrek et al., 2016; Everhart et al., 2010). *Xiphactinus* fossils can be found as far south as Texas and Mexico (Bardack 1965; Stovall, 1933) and as far north as Canada (Vavrek et al., 2016; Bardack, 1965; Stovall, 1933). These fossils most often belong to the species *X. audax* (Leidy 1873; Leidy, 1870). *X. audax* is one of two currently recognized species of *Xiphactinus*, though at least ten species have been recognized at various times (Bardack, 1965; Hay, 1898). The second species, *X. vetus*, is more commonly found along the Atlantic coast and can be differentiated from *X. audax* by laterally flattened dentition and posterior carinae on the teeth—in contrast to the rounded, bullet-shaped teeth of *X. audax* (Vavrek et al., 2016; Schwimmer et al., 1997). *X. vetus* was not included in this study due to sparse fossil material composed almost exclusively of isolated teeth and vertebrae (Vavrek et al., 2016).

Ecologically, *X. audax* was an elongate, pelagic predatory fish that likely preyed opportunistically on other large ichthyodectid fish (Beamon, 2001). Stomach contents are known from numerous specimens and most often show a prey of *Gillicus*—another

smaller ichthyodectid fish—swallowed head-first. The number and consistency of these feeding remnants imply not only preferred prey, but provide insight into the preferred feeding style of *X. audax* (Bardack, 1965, Walker, 2006).

Megalops is an extant genus of elopiform fish represented by two species—*M. cyprinoides* (oxeye) and *M. atlanticus* (Atlantic tarpon). *M. atlanticus*, the focus of this study, is native to the Gulf of Mexico and both East and West Atlantic coasts, with a small population in the Pacific Ocean via the Panama Canal (Adams et al., 2012). *M. atlanticus* is a popular sport fish and can reach lengths of over 2.0 m (Grubich, 2001). They lack teeth as adults and feed primarily on schooling fish and crustaceans using suction feeding (Westneat, 2005; Grubich, 2001; Whitehead & Vergara, 1978). *M. atlanticus* is also notable in its complex ontogenetic development, including three distinct larval stages during which time offspring share little resemblance to their adult form (Wade, 1962).

M. atlanticus and *X. audax* share a number of characteristics in both their cranial and post-cranial anatomy. Both species share an elongate body, a deeply-forked caudal fin, similarly constructed hemal arches, and a caudally situated dorsal fin—all characteristics of an opportunistic ambush predatory lifestyle (Cavender, 1966; Beamon, 2001; Grubich, 2001; Taverne, 2008; Osborn, 1904). Cranially, both species share an antero-caudally compressed skull, deep mandible, and a forward-slung quadrate-articular articulation, resulting in a strongly supraterminal mouth—features which imply a life-history strategy of hunting prey from below (Taverne, 2008; Grubich, 2001; Gregory, 1933). Despite this configuration, *M. atlanticus* does still prey on benthic organisms with

some frequency (Adams et al., 2012; Whitehead & Vergara, 1978). Similarities in the crania and post-crania have resulted in many formal and informal comparisons of the two species, with *X. audax* being referred to as a ‘bulldog fish,’ ‘Cretaceous tarpon,’ or ‘fanged tarpon’ in both popular media and academic descriptions (Taverne, 2008; Hay, 1898; pers. obs.). These similarities have not been lost in taxonomic analysis, with Gregory (1933), Hay (1898), and Cope (1871a) uniting both genera in the now-defunct order of basal teleosts Isospondyli.

Cope (1871b) originally placed *Portheus*—later synonymized with *Xiphactinus* (Hay, 1898)—into the family Saurodontidae (Dana et al., 1872). More contemporary cladistic analyses have placed *Xiphactinus* alternatively within Chirocentridae (Bardack, 1965), which has been actively disputed based on post-cranial characters (Cavender, 1966), or Ichthyodectidae (Vavrek et al., 2016; Murray & Cook; 2016; Everhart, 2010; Patterson & Rosen, 1977; Bardack, 1969; Cavender, 1966; Crook, 1892), which is the current consensus. Ichthyodectidae has been alternatively placed within Ichthyodectiformes (Bardack, 1969) or Teleostei *incertae sedis* (Nelson, 1973). *Megalops* belongs to the family Megalopidae within the order Elopiformes (Adams et al., 2012). Bardack (1969) united both Elopiformes and Ichthyodectiformes into the superorder Elopomorpha, an intermediate grade of basal teleosts between the more basal Osteoglossomorpha and the more derived Clupeomorpha (Lauder & Liem, 1983). The placement of *Xiphactinus* into Elopomorpha is dubious, however, as the sole synapomorphy supporting the monophyly of this clade is the presence of the leptocephalus larval stage—a stage unknown in fossil *Xiphactinus* material (Grubich,

2001). Nonetheless, phylogenetic analysis has consistently supported the basal arrangement of both Ichthyodectiformes and Elopiformes, with Arratia and Tischlinger (2010) recovering a cladogram placing Ichthyodectiformes as basal to Elopiformes, and Maynrick et al. (2015) recovering a cladogram with both orders in a polytomy with each other and a third order, Crossognathiformes. In both formal systematic analyses including Ichthyodectiformes and Elopiformes, both orders fell out basal to other basal ‘grades’ of teleosts, including Osteoglossomorpha and Clupeomorpha—contradicting previous placements of these orders (Lauder & Liem, 1983). However, neither Arratia and Tischlinger (2010) nor Maynrick et al. (2015) incorporated *Xiphactinus* or other WIS ichthyodectiforms into their analyses, instead only including older Jurassic members of the clade. How these orders would resolve if WIS ichthyodectids were included is unknown.

The complex taxonomy of these fish is important because the close association of Ichthyodectiformes and Elopiformes as basal teleosts may make it tempting to assume the shared cranial morphology between *X. audax* and *M. atlanticus* is due to shared ancestry. However, Elopidae—the sister group of Megalopidae—as well as basal members of Elopiformes such as *Anaethalion* lack many of the seemingly convergent cranial characteristics present in Megalopidae mentioned previously, suggesting that these features independently evolved within Megalopidae (Maynrick, 2015; Nelson, 1973). While this comparison is useful in interpreting the results in the following analyses, it is not a true replacement for an ancestral state reconstruction to determine the last common ancestor of *Xiphactinus* and *Megalops*. Though beyond the scope of this study, an

ancestral state reconstruction is a necessary component in assessing the selective trajectory of these taxa to differentiate homoplasy from shared common ancestry.

MATERIALS AND METHODS

Institutional Abbreviations

FHSM: Fort Hays State University's Sternberg Museum of Natural History, Hays, KS

AMNH: American Museum of Natural History, New York, NY

USNM: Smithsonian National Museum of Natural History, Washington, D.C.

YPM: Yale Peabody Museum of Natural History, New Haven, CT

NCSM: North Carolina Museum of Natural Sciences, Raleigh, NC

TNHC: The University of Texas at Austin Biodiversity Center, Austin, TX

UF: Florida Museum of Natural History, Gainesville, FL

Materials

Cranial material of six specimens of *Xiphactinus audax* (AMNH FF-1951; FHSM VP-333; FHSM VP-699; USNM V11554; USNM V-11653; YPM VP-56875) and six specimens of *Megalops atlanticus* (AMNH 211548-SD; NCSM 45757; TNHC 62473; UF 10674-S; USNM 21554; USNM 260337) were selected for 2D and 3D reconstruction and analysis. Selected specimens were in various states of articulation, from fully disarticulated to fully articulated (Table 1). In all cases, analyzed specimens included the following elements: braincase (including all articulations relevant to mandibular and suspensorial elements), mandibular arch (premaxilla, maxilla, dentary, autangular,

dermangular, retroarticular, coronomeckelian), palatal elements (palatine, endo or mesopterygoid, metapterygoid, ectopterygoid), and suspensorial elements (hyomandibular, quadrate). The symplectic and supramaxillae were excluded due to their fragility and tendency not to preserve in fossil specimens. Additionally, when these elements were preserved, they were too small and thin to scan and maintain an accurate model boundary. Some information about the angle of the symplectic can be inferred from the shape and angle of its articulation with the quadrate. The symplectic projects ventrally from the hyomandibular and extends into a dorsal groove on the quadrate, strengthening it against mandibular stresses (Gregory, 1933). The supramaxillae serve in part as the attachment point for the *ligamentum maxilla-mandibulare anterius*, one of two ligaments directly connecting the upper jaw to the lower jaw in teleosts (Vrba, 1968). The exclusion of these elements has implications for interpreting feeding mechanics, which are further discussed below (see Discussion).

Only large specimens of both species were used in analysis, with size used as a proxy for age to reduced ontogenetic bias during analysis. When the standard length (SL) of a specimen was not known, it was estimated from the length of the cranium as a proportion of the overall body length (Table 1). All *M. atlanticus* specimens had SL greater than 120 cm, representing the average threshold for sexually mature individuals (Adams et al., 2012). *M. atlanticus* undergo considerable ontogenetic change during larval development, but the last stage of their extreme larval metamorphosis occurs between 40-130 mm (Wade, 1962). By sexual maturity, *M. atlanticus* have undergone the most substantial phase of their ontogeny and have achieved adult proportions.

Approximation of sexual maturity is more difficult to assess in *X. audax* due to a lack of modern ichthyodectid representatives. However, all examined specimens had estimated SL greater than 300 cm. While the size threshold for sexual maturity in *X. audax* is unknown, it is presumed for the purposes of this study that such large individuals have already undergone a majority of their ontogenetic metamorphosis and have achieved adult proportions. Adult proportions might be inferred by analyzing the *X. audax* specimens and making shape comparisons based on specimen size. Such an analysis was not performed for this study, however, as the small sample size would prohibit reasonable interpretations of differences in maturity versus normal population variation.

Data Collection

Specimen Digitization

Specimens were scanned using a Creaform Go!SCAN Model 50 structured light 3D surface scanner. This model of scanner projects a pattern of visible structured light onto the target and uses a pair of cameras to detect deformations in this pattern. The associated software, VXelements, construes this deformation into a mesh called a 3D scan. This mesh is composed of fundamental polygonal surfaces called triangles. VXelements is composed of two modules—VXscan, the module used for specimen scanning, and VXmodel, the module used for post-processing of 3D mesh. Scans were performed at a resolution of 0.50 mm, the highest resolution possible with the hardware. 3D models were produced from these scans in Wavefront (.obj) and stereolithography

(.stl) formats. Analyses used .stl files due to their universal compatibility with most 3D software. Scanning involved taking multiple, individual 3D scans of a specimen from multiple angles, then merging these volumes into a single mesh using the *Merge* function in VXscan. A single model consists of one to five individual 3D scans.

Post-processing of models was performed in the VXmodel module. For most elements, post-processing consisted of minor mesh-cleaning using editing tools available in the software. This included filling small holes, removing stray data dissociated from the main body of the specimen, removing spikes and creases in the mesh, and removing non-manifold triangles (polygons that would prevent the model from existing within real world geometry). In cases of exceptionally heavy files, a decimation function was performed on the offending model. This function removed triangles without altering the accuracy of the mesh boundary, reducing file size and processing times during analysis.

Specimens were also photographed using a Canon EOS Rebel t5 camera with a Canon 18-55 mm macro lens. All images were scaled, but lighting conditions varied among photographs. These photographs were not used in analysis, but rather for reference during reconstruction and landmark placement.

Specimen Reconstruction

For 3D comparative analysis of the feeding morphology of the two fish species, partially complete and disarticulated skulls had to be reconstructed in three dimensions. Reconstructions were performed in the VXmodel module of VXelements. This module

permits importation of individual 3D models and adjustment of their relative alignments. For disarticulated skulls, models of individual elements were imported and aligned into their anatomically correct articulations (based on Gregory, 1933). For fossil specimens with obvious taphonomic damage, fractures were reset into correct position along fracture planes using the VXmodel editing tools. Irreparable specimens were excluded from analysis. In the case of specimens with missing elements, or specimens with only one half of the skull exposed due to mounting for exhibition (i.e. FHSM VP-333), elements from the available side of the individual were mirrored using the *Mirror* function in VXmodel to generate a complete skull for analysis. Most teleosts, including ichthyodectids and megalopids, have bilaterally symmetrical crania as adults (Gregory, 1933), so using well-preserved, mirrored elements introduced minimal bias.

In cases of plaster-mounted fossil specimens, parts of some elements were obscured by overlying elements—most often portions of the dentary were concealed by the overlying maxilla. To generate complete reconstructions, other specimen models were used to patch obscured sections, forming composite elements. This was done by trimming sections of an appropriately scaled model of the same element from a different specimen and merging it into the missing section. Using this method, visible portions of the original element (e.g. a visible anterior and posterior portion of a dentary) were united using their visible boundaries for reference. Only the obscured sections were reconstructed using this method—not broken regions—and inferences regarding the proportions of the original elements were not made. Anterior and posterior portions of a reconstructed element retained their original relative proportions and were united into a single composite

element. This procedure was done to ensure all cranial elements were complete and could be assessed in various software (discussed below) which often prohibit the analysis of incomplete 3D models. Landmarks were not placed along these composite sections. This was done to prevent non-independence in downstream analyses resulting from the same element being analyzed twice, which would bias the results and obscure accurate shape analysis of the reconstructed specimen.

To ensure consistent comparison among reconstructed skulls, all skulls had their jaws positioned with a standard jaw angle, gape width, and gape size (Fig. 1). Establishing and maintaining these proportions ensured that the highly variable mouth gape remained consistent relative to the size of the cranium in each specimen, helping reduce bias introduced from differences in mouth position. These proportions fall within the normal range of jaw motion for both species based on feeding analysis of *M. atlanticus* (Grubich, 2001) and the movement of elements along their articular surfaces in *X. audax* (pers. obs.). These proportions also allow for maximum visibility of mandibular and suspensorial elements for both 2D and 3D analysis.

The upper jaw of all specimens was oriented at an angle of 60° from a plane drawn through the center of the occipital condyle. The line forming the angle with this plane was drawn from the anteroventral-most point of the premaxilla, to the posterior-most point of the maxilla, in left lateral view (Fig. 1A). Gape size was measured from the anteroventral-most point of the premaxilla to the anterodorsal-most point of the dentary, along the axis of rotation of the lower jaw when articulated with the quadrate. Gape size was standardized at 0.5 times the length of the neurocranium, as measured from the

anterior point of the dermethmoid, to the posterior point of the base of the supraoccipital ridge (*M. atlanticus*) or crest (*X. audax*) (Fig. 1A). Gape width was calculated between the articular condyles of the quadrates at the ventral-most point of the suspensorium. Gape width was standardized at 1.25 times the widest point of the braincase, measured from the lateral-most point between the left and right pterotics (Fig. 1B). Cranial elements of fossil specimens were never forced into place or digitally altered to fit together.

A left lateral profile image of each reconstructed model was printed, and tracing paper was used to create line drawings of the reconstructed specimen. These drawings were digitally scanned and sharpened for clarity in Adobe Illustrator CS6. These line drawings were used for 2D analysis.

Data Analysis

A total of four treatments were carried out in this study: 2D analysis, 3D analysis, outlier adjusted 2D analysis, and outlier adjusted 3D analysis. A quantile-quantile plot of the samples was generated in the R package *mvoutlier* (R Core Team, 2017; Filzmoser, 2018) to investigate for outliers in the dataset. Extreme outliers were removed for the outlier adjusted analyses (Table 1).

Landmark placement

Landmark-based GM methods rely on statistical analysis of landmarks carrying Cartesian coordinates placed on biologically informative features of specimens. To place landmarks in 2D, methods outlined in Zelditch (2012) were followed, using the Stony Brook TPS family of software. Line drawings were uploaded into the program tpsUtil ver. 1.74 (Rohlf, 2019) to generate a TopSpeed (.tps) file containing image data. This file was then imported into the program tpsDig2 ver. 2.31 (Rohlf, 2010), where landmarks were placed using the *Digitize landmarks* function. Fourteen landmarks marked homologous points among specimens, concentrated on the mandibular arch, palatal elements, and suspensorium, with some placed along the neurocranium to better outline the full shape of the skull (Fig. 2A). Selected points generally defined the anterior- and posterior-most points of mandibular elements and articulations, and were selected to define the shape and relative placement of these elements.

The procedure for landmark placement in 3D reconstructed models differed from 2D landmark placement. Points representing landmarks were manually placed using the GM software Landmark ver. 3.0.0.6 (Wiley et al., 2005). Landmark placement was mirrored from the 2D analysis, meaning landmarks were placed on the same homologous points between both treatments. However, 24 landmarks were placed in 3D rather than 14. Landmarks 1 through 4 were placed along the midline and were not mirrored. Landmarks 5 through 14 were mirrored onto the right side of the model (Fig. 2B). The spatial Cartesian coordinates for both 2D and 3D landmarks were exported as point (.pts)

files, which was then formatted for use in the R package geomorph (R Core Team, 2017; Adams & Otárola-Catillo, 2013) following Sokal & Rohlf (2009).

General Procrustes Superimposition and Principal Components Analysis

General Procrustes superimposition (GPA) is a statistical procedure used in GM where the sum of squared distances among all homologous landmark clusters is minimized (Adams et al., 2004). This procedure rotates, translates, and scales specimen landmarks and superimposes them, ensuring the effects of size and rotation are accounted for during statistical analysis (Adams et al., 2004; Slice, 2007). For both 2D and 3D analysis GPA was carried out in the R package geomorph (R Core Team, 2017; Adams & Otárola-Catillo, 2013), using the *gpagen* function. These superimposed data were then used to perform a principal components analysis (PCA) using the *plotTangentSpace* function. PCA is an ordination technique where variables in multidimensional space are ordinated along arbitrarily generated eigenvectors called principal component axes, or just principal components (PC), and compressed into fewer dimensions for ease of analysis. PC axes are unitless, linear combinations of the original input variables with each axis orthogonal to the last in multidimensional space (Paliy & Shankar, 2016). PC axes are organized based on descending order of explained variation between variables: PC1 explains the most variation, PC2 the second most, etc. Different PC axes generally explain different sources of variation among variables (Zelditch et al., 2012). In this study, each point represents an individual specimen within PC space and specimens cluster based on similarity in shape. PCA was used to assess the similarity and

dissimilarity of the crania of the two species in both 2D and 3D through their relative positions in PC morphospace. Deformation grids were generated alongside the 2D PCA that illustrate the shape variation defined by a given PC axis and the landmarks responsible for that shape variation. In 3D analyses deformation grids could not be produced and shape information was instead assessed using 3D point clouds of the landmarks, which served a similar function.

PC scores (the PC morphospace coordinates of each specimen) and PC loadings (the amount of relative variation each PC axis explains) were exported as Microsoft Excel Open XML Spreadsheet (.xlsx) files. PC scores for each PC axis were then multiplied by their loadings on each axis. These weighted data were formatted following Sokal and Rohlf (2009), converted into a tab delimited text (.txt) file, and imported back into R for additional analyses. This weighting procedure prevented downstream analyses from assuming each PC explained the same amount of relative variation, ensuring an emphasis on more meaningful sources of variation and eliminating bias towards less meaningful sources of variation. Only PC axes that contributed to the first 90% of variation were retained and assessed. In all four treatment, this equated to the first four PC axes.

Discriminant Function Analysis

Discriminant function analysis (DFA) is an eigenvector technique similar to PCA, but generates clusters similar to SAHN clustering (described below). Unlike SAHN

clustering, which produces groups based on similarity, DFA looks for pre-existing groups in the data and maximizes between-group differences while minimizing within-group differences. DFA was performed in the R package MASS (Venables & Ripley, 2002) using the function *lda*. DFA results were used alongside PCA and SAHN to strengthen interpretations regarding shape differences in the crania of the two fish species.

SAHN Clustering Analysis

Sequential, agglomerative, hierarchical, non-overlapping (SAHN) clustering is a clustering technique where a similarity or distance matrix is grouped sequentially in a manner that minimizes within group differences and maximizes between group differences. The output for a SAHN clustering procedure is a dendrogram, a branched diagram representing a two dimensional flattening of multidimensional space. Specimens are organized within this space based on statistical similarities, similar to an ordination. It is read like a cladogram, with branch proximity indicating a closer relationship—in this case similarity in geometry (Müllner, 2011). Despite the visual similarities to a cladogram, it must be stressed that SAHN clustering is not a systematic technique. SAHN clustering was used alongside PCA and DFA to strengthen interpretations regarding shape differences in the crania of the two fish species.

Standard Euclidean distance matrices of both the 2D and 3D data were produced in the R package *vegan* (Oksanen et al., 2019) from the weighted PC data using the function *vegdist*. SAHN cluster analysis was performed on this distance matrix using the

hclust function. Average link clustering (UPGMA) was the chosen clustering algorithm. UPGMA generates groups by comparing the distance to the next object to be clustered from the centroid of previous clusters rather than a single object in a previous cluster (Müllner, 2011). This more dynamic method of clustering produces generally better results with less chaining. The cophenetic value, which indicates how well the cluster matches variation in the original data, was calculated using the *cophenetic* function. Cophenetic values closer to 1 indicate a closer match between the original data and the clustered data.

Multi-response Permutation Procedure

A multi-response permutation procedure (MRPP) is a nonparametric statistical procedure developed to test for differences among groups. This procedure works by calculating a delta (δ) value (observed δ) from a distance matrix, then calculating the probability of a smaller δ value (expected δ). From these values, the test statistic T , an agreement statistic A , and a p value are generated. T describes the separation between groups, with more negative values indicating a greater degree of separation. A describes the degree of within-group homogeneity, with a value of 1 indicating all specimens within a group are identical. Lower values indicate correspondingly less homogeneity, with values <0 indicating specimens within groups are less homogenous than would be expected by random chance. (McCune & Grace, 2002).

Standard Euclidean distance matrices of both the 2D and 3D data were produced following Zimmerman et al. (1985) in the R package *vegan* (Oksanen et al., 2019) from the weighted PC data using the function *vegdist*. MRPP was carried out using the *mrpp* function.

RESULTS

Outlier Analysis

Outlier testing on the dataset recovered FHSM-VP 699 and YPM VP-56875 as extreme outliers. These specimens were removed from the analysis for both the 2D and 3D outlier adjusted analysis. TNHC 62473 was also recovered as an outlier, but far less so than the previously mentioned specimens. Because of this, TNHC 62473 was retained in the outlier adjusted analyses.

Principal Components Analysis

The 2D shape analysis shows strong within-species grouping and between-species separation in morphospace along PC1 (Fig. 3A). PC1 accounts for 68.2% of the shape variation. All specimens of *M. atlanticus* fall out negatively along PC1 and all specimens of *X. audax* fall out positively along PC1 with no ambiguity in these groupings. The *M. atlanticus* grouping is, however, more tightly clustered along PC1 while the *X. audax* grouping is more diffuse, indicating a weaker in-group association in *X. audax*. Shape variation along PC1 is mediated primarily by differences in the size of the premaxilla, the proportions of the quadrate, and the angle of the mandibular symphysis. Positive values along PC1 are associated with a broader premaxilla, a relatively shorter quadrate-metapterygoid articulation, and a caudally deflected mandibular symphysis. Negative values along PC1 are associated with a more compressed premaxilla, a longer quadrate-metapterygoid articulation, and an anteriorly deflected mandibular symphysis. The

position of the posterior maxilla relative to the articular also contributes to variation along PC1, with more positive values reflecting a greater distance between the two elements. When outliers FHSM VP-699 and YPM VP-56875 are removed, PC1 explains 73.0% of the shape variation (Fig. 3C). Both the groupings and the sources of shape variation along PC1 remain the same between unadjusted and outlier-adjusted analyses.

The 3D shape analysis shows strong within-species grouping and between-species separation along PC1 (Fig. 4A). PC1 accounts for 66.1% of the shape variation. All *M. atlanticus* specimens fall out negatively along PC1 and all *X. audax* specimens fall out positively, emphasizing the strong separation between species groups. The *M. atlanticus* group is tightly clustered along PC1, with TNHC 62473 representing a potential outlier. The *X. audax* group is clustered more diffusely, with FHSM VP-699 and YPM VP-56875 appearing as notable outliers as in the 2D results. Shape variation along PC1 appears to be primarily mediated by differences in the size of the premaxilla, the distance between the dermethmoid and the palato-premaxillary articulation, the angle of the symplectic, the distance between the posterior maxilla and the articular, the angle of the mandibular symphysis, and the breadth of the buccal cavity in anterior aspect. Positive values along PC1 are associated with a broader premaxilla, a greater distance between the dermethmoid and the palato-premaxillary articulation, a more vertically-oriented symplectic articulation, greater distance between the anterior maxilla and the articular, a caudally-deflected mandibular symphysis, and a narrower buccal cavity. Negative values along PC1 are associated with a dorsoventrally compressed premaxilla, a shorter distance between the dermethmoid and the palato-premaxillary articulation, a more anteriorly-

deflected symplectic articulation, a shorter distance between the posterior maxilla and the articular, an anteriorly-deflected mandibular symphysis, and a broader buccal cavity.

When outliers FHSM VP-699 and YPM VP-56875 are removed, PC1 explains 71.0% of the shape variation (Fig. 5A). Both the groupings and the sources of shape variation along PC1 remain the same between unadjusted and outlier-adjusted analyses.

PC2 accounts for 11.0 % of the shape variation in the 2D analysis (Fig. 3B).

Along PC2, between-species groups did not appear and specimens of *M. atlanticus* and *X. audax* fall out both positively and negatively along this axis. The *M. atlanticus* group is well-defined, though TNHC 62473 appears as a potential outlier within this species. The *X. audax* group is much more diffuse with *M. atlanticus* forming a nested group within the much broader *X. audax* group. Shape variation along PC2 appears to be mediated primarily by differences in the angle of the dorsal hyomandibular articulation, angle of the quadrate-metapterygoid articulation, distance between the posterior maxilla and the articular, and the angle of the mandibular symphysis. Positive values along PC2 are associated with a shallower angle of the dorsal hyomandibular articulation, a steeper angle of the quadrate-metapterygoid articulation, a greater distance between the posterior maxilla and the articular, and a caudally deflected mandibular symphysis. Negative values along PC2 are associated with a steeper angle of the dorsal hyomandibular articulation, a shallower angle of the quadrate-metapterygoid articulation, a shorter distance between the posterior maxilla and the articular, and an anteriorly deflected mandibular symphysis. When outliers FHSM VP-699 and YPM VP-56875 are removed,

PC2 explains 9.7% of the shape variation (Fig. 3D). The between-species grouping remains ambiguous, and the sources of shape variation remains largely the same.

PC2 accounts for 12.1% of the shape variation in the 3D analysis (Fig. 4B). No distinct between-species group separation occurs along PC2. *M. atlanticus* specimens are more tightly clustered than *X. audax* specimens and form a nested group within the more diffuse *X. audax* group. Both species fall out positively and negatively along PC2. Shape variation along PC2 is primarily mediated by the size of the premaxilla, the angle of the quadrate-metapterygoid articulation, the length and angle of the symplectic, the distance between the posterior maxilla and the articular, and the angle of the mandibular symphysis. Positive values along PC2 were associated with a larger premaxilla, a steeper quadrate-metapterygoid articulation angle, a shorter and more vertically-oriented symplectic articulation, a greater distance between the posterior maxilla and the articular, and a caudally-deflected mandibular symphysis. Negative values along PC2 are associated with a dorsoventrally compressed premaxilla, a shallower quadrate-metapterygoid articulation angle, a longer and more anteriorly-deflected symplectic articulation, a shorter distance between the posterior maxilla and the articular, and an anteriorly-deflected mandibular symphysis. When outliers FHSM VP-699 and YPM VP-56875 are removed, PC2 accounts for 10.5% of the shape variation (Fig. 5B). Between-species groupings remain indistinct, with *M. atlanticus* specimens again forming a tighter cluster among the more diffuse *X. audax* specimens. The sources of variation remains largely the same along PC2 between unadjusted and outlier-adjusted analyses. There is,

however, a less substantial difference in the angle of the mandibular symphysis between negative and positive PC2 loadings after removing the outliers.

Discriminant Function Analysis

One linear discriminant (LD1) is generated from both the 2D and 3D DFA. DFA is able to successfully assign specimens to their correct species group 100% of the time in both analyses, indicating a strong degree of separation between the species groups along LD1 (Fig. 6A,B). When outliers FHSM VP-699 and YPM VP-56875 are removed, these results remained the same (Fig. 6C,D).

SAHN Clustering Analysis

The 2D and 3D SAHN clustering analyses both generate dendrograms forming two well-separated clusters for *M. atlanticus* and *X. audax* (Fig. 7A,B). VP-699 and YPM VP-56875 appear as notable outliers in these analyses as well, forming distinct, separate pairs within the *X. audax* cluster. After removing the outliers VP-699 and YPM VP-56875, the *M. atlanticus* and *X. audax* clusters remain strongly separated in both 2D and 3D analyses (Fig. 7C,D). The 2D unadjusted cophenetic value is 0.907, indicating a parity of 90.7% between the input data and the generated dendrogram. The 2D outlier-adjusted cophenetic value is 0.906, indicating a parity of 90.6% between the input data and the generated dendrogram. There is notably more chaining in the 2D outlier-adjusted dendrogram, and some difference in specimen association between the 2D unadjusted and

outlier-adjusted analyses. Specifically, USNM 260337 is less strongly associated with USNM 21554 in the outlier-adjusted dendrogram. The cophenetic value for the 3D unadjusted analysis is 0.909, indicating a parity of 90.9% between the input data and the generated dendrogram. The *M. atlanticus* and *X. audax* clusters remain strongly defined after removal of VP-699 and YPM VP-56875. The 3D outlier-adjusted cophenetic value is 0.900, indicating a parity of 90.0% between the input data and the generated dendrogram. There is some change in the association between the 3D unadjusted and outlier-adjusted analysis. UF 10674S forms a stronger association with USNM 21554 and FHSM VP-333 forms a stronger association with USNM V 11653 in the outlier-adjusted analysis.

Multi-response Permutation Procedure

All MRPP values are concatenated in Table 2. 2D MRPP analysis shows that the degree of separation between groups is greater than that expected by chance, indicating a significant difference between the *M. atlanticus* and *X. audax* species groups ($p = 0.002$). Species groups also have a high degree of within-group similarity and a high degree of between-group separation ($A = 0.774$, $T = -7.34$). When the outliers FHSM VP-699 and YPM VP-56875 are removed, the difference between species groups remains significant, though less significant than the unadjusted analysis ($p = 0.006$). Species groups in the outlier-adjusted analysis also have a greater degree of within-group similarity, but reduced between group separation than the unadjusted analysis ($A = 0.856$, $T = -5.76$). However, between-group separation still remains high in the outlier-adjusted analysis.

3D MRPP analysis also finds a significant difference between the *M. atlanticus* and *X. audax* species groups ($p = 0.002$). Species groups again maintain a high degree of within-group similarity and between-group separation comparable to the unadjusted 2D results ($A = 0.758$, $T = -7.34$). When the outliers FHSM VP-699 and YPM VP-56875 are removed, there is still significant difference between the species groups, though less significant than in the unadjusted analysis ($p = 0.005$). 3D outlier-adjusted groups also show a greater degree of within-group similarity when compared to the unadjusted 3D analysis and reduced between-group separation ($A = 0.823$, $T = -5.86$).

DISCUSSION

All analyses in both 2D and 3D show discrete morphospace occupation between both species (Figs. 3-7). The qualitative dissimilarity illustrated in the PCA, DFA, and SAHN cluster analyses is corroborated by the MRPP, which found a significant difference ($p < 0.05$) in the shape of the jaw morphology between species among all treatments, with the significance of this separation decreasing slightly after the removal of the outlier specimens FHSM VP-699 and YPM VP-56975 (Table 2). This means that *X. audax* and *M. atlanticus* occupy distinct regions of morphospace in relation to feeding morphology, corroborated by their known feeding habits (discussed below), suggesting *M. atlanticus* is a poor modern analog for *X. audax*. These analyses also produce nearly identical results in both 2D and 3D treatments. This fact suggests that there is little to no advantage to performing landmark-based GM analysis on 3D models versus 2D images when interest in quantifying the complexities of 3D structures is minimal.

The outlier specimens do not represent the largest or smallest *X. audax* individuals in the dataset, and were not notably more taphonomically altered than non-outlier specimens. This rules out ontogeny or taphonomy as culprits for their status as outliers. These specimens may fall within a normal range of intraspecific variation for *X. audax*, which is not being properly represented due to small sample size. Alternatively, these specimens may show evidence of some other form of population variation, such as sexual dimorphism, or may represent a cryptic species. These conclusions are beyond the scope of this study, but may be beneficial future research.

The PCA provides further insight into the source of the shape difference between species. In all treatments, PC1 represents the sole axis of between-species separation in morphospace, with other axes showing shared morphospace occupation. However, >65% of the variation was explained by PC1 in all analyses, indicating that a majority of the variation described dissimilarity in shape rather than similarity (Figs. 3A; 4A). This variation increases to >70% after the removal of the outliers (Figs. 3C; 5A). PC1 has eigenvalues ranging between 7.09 and 8.18 (Table 3), making it by far the most informative axis to interpret. By contrast, PC2 has eigenvalues ranging between 0.97 and 1.44. PC3 and PC4 all had values <1. Axes with eigenvalues below 1 explain less variation than the input variables, making them generally uninformative. For these reasons, axes 3 and 4 will not be discussed further.

There is consistency in the specific sources of variation along PC1 among all four treatments (with the exception of variation resulting from cranial width that could not be measured in the 2D analyses). *M. atlanticus* has a small, quadrangular premaxilla, whereas *X. audax* has a larger, more ovular premaxilla. The premaxilla of *X. audax* is also strongly interdigitated to the maxilla, in contrast to the premaxilla of *M. atlanticus* (Osborn, 1904; Gregory, 1933 pp. 139-141, 143; Bardack, 1965). These differences in premaxillary arrangement reflect differences in prey type and acquisition between the two fish species. The interdigitated premaxilla-maxilla complex of *X. audax* produces an upper jaw that is more resistant to fracture and dislocation—one of a suite of features useful in resisting stresses when feeding opportunistically on large, thrashing prey (Beamon, 2001, Bardack, 1965). The more quadrangular and compressed premaxilla of

M. atlanticus contributes to a more gracile upper jaw arrangement reflecting its dietary habits, with adults feeding primarily on small schooling fish, worms, and crustaceans (Whitehead & Vergara, 1978; Adams et al., 2012).

The distance between the posterior maxilla and the articular is another feature that varies consistently between both species in all treatments along PC1. This difference is indicative of a greater length in the maxilla of *M. atlanticus*, resulting in a maxilla that draws closer to the articular in life position. During suction feeding, the maxilla is used as a lever to expand the mouth, with longer maxillae indicating stronger suction forces and therefore a greater reliance on this method of feeding (Westneat, 2004). The relatively shorter and more robust maxilla of *X. audax* and the less kinetic upper jaw indicates *X. audax* relied less on the suction forces during feeding than does *M. atlanticus* (Bardack, 1965). In modern long-toothed fish species, suction feeding is used to aid a biting capture and it may be inferred that this style of feeding applied to *X. audax* as well (Westneat, 2005). This inference is corroborated by known prey size and feeding behavior of *X. audax* and other related ichthyodectids, which feed on large prey items head-first, much like the modern long-fanged *Chirocentrus* (Bardack, 1965; Luther, 1985; Walker, 2006; Everhart et al., 2010). However, no comprehensive study on the feeding biomechanics of *Xiphactinus* currently exists. While they certainly employed suction feeding—a feature plesiomorphic to teleosts—this study indicates that suction may not have been as critical to the feeding strategy of *X. audax* as it is to large, predatory, pelagic fish today (Westneat, 2004; Westneat, 2005), as evidence both by their relatively akinetic premaxillae and relatively short, robust maxillae.

The angle of the mandibular symphysis also varies between species, with *X. audax* having a strong caudal deflection of the anterior dentary, while *M. atlanticus* has a moderate anterior deflection of the anterior dentary forming a chin-like protrusion. The caudal deflection present in *X. audax* is a condition common in extant teleosts bearing dental fangs, including members of Chirocentridae, Alestidae, and Cynodontidae (Gregory, 1933 pp. 142, 184; Bardack, 1965; Westneat, 2004). This condition is even present in the fanged larval forms of *M. atlanticus*, but is lost during ontogeny (Wade, 1962), reflecting a lack of adaptive advantage or necessity when large teeth are not present. It may be hypothesized, therefore, that this condition in *X. audax* is related to the eruption and accommodation of large anterior thecodont teeth in the dentary and/or prey handling. Whether there is some biomechanical advantage to this condition during feeding is unclear and requires additional research.

Also peculiar in the two fish species included in this study is the shape and angle of the mandibular symphyses. Both species have relatively deep symphyses, indicating a strong connection between the left and right dentary resulting in relatively deep mandibles. The presence of such a deep symphysis in *M. atlanticus* is curious as adult *M. atlanticus* do not feed on large or particularly strong prey (Whitehead & Vergara, 1978; Adams et al., 2012). This suggests that resisting feeding stresses is a poor explanation for such a deep and seemingly akinetic dentary association in *M. atlanticus*. This deep mandible is a feature of adult tarpon and is not present in the toothed or toothless larval and subadult forms, refuting any neotenic or ontogenetic explanation. A phylogenetic explanation may be hypothesized, as both extant megalopids (*M. atlanticus* and *M.*

cyprinoides) share this condition (Wade, 1962). Other elopiforms however, including members of the sister family Elopidae and the more basal *Anaethalion*, lack such a deep symphysis. Instead, they exhibit a narrower, more terminal jaw, and a less robust mandible (Whitehead & Vergara, 1978; Maynrick et al., 2015). The deep symphysis appears to be synapomorphic rather than plesiomorphic to Megalopidae. A final hypothesis to consider is that the deep symphysis of *Megalops* is related to feeding, but evolved under a different selective regime than the deep symphysis of *X. audax*. The deep mandible of *Megalops* increases the buccal capacity of these fish during feeding, enhancing their ability to suction feed and intake food during the expansive phase of suction feeding. This would further reduce water pressure in the mouth and increase the force of the suction created during the expansive phase (Westneat, 2005). This explanation is also supported by the relative kinesis of the upper jaw (particularly in the ball-and-socket arrangement of the maxillo-palatine articulation) and length of the maxilla of *M. atlanticus* which are both characteristics related to suction feeding efficiency (Bardack, 1965; Grubich, 2001; Westneat, 2004; Westneat, 2005). By contrast, a deep mandibular symphysis is a sensible solution to resist forces imparted by large prey items in *X. audax*, much like their strongly interdigitated premaxillae discussed above. Due to the relative lack of jaw kinesis, obvious reliance on prominent, deeply-socketed teeth, and clear preference in large individual prey items, it is unlikely that the evolution of a deep symphysis in *Xiphactinus* was mediated primarily by selection towards suction feeding efficiency, as seems to be the case in *Megalops*. The more parsimonious explanation is that the deep symphysis in *X. audax* is an adaptation for a strengthened jaw and to anchor deeply rooted, thecodont dentition for feeding on relatively large, strong

prey items. This is further corroborated by the previous results from the size and shape of the maxillary and premaxillary elements.

The similarity in mandibular symphysis depth between *X. audax* and *M. atlanticus* is noteworthy because it highlights the importance of distinguishing between functional convergence and structural convergence. This feature—while likely having evolved independently in both Megalopidae and Ichthyodectidae—seems to have structurally converged incidentally and not due to shared ecological pressures. While there are finite solutions to the same functional problems resulting in organisms trending towards the same adaptive structural optima (Ingram & Mahler, 2013; Mahler et al., 2013; Arbuckle et al., 2014), the same structural solutions may also be used to overcome different functional problems. Being cognizant of this fact is valuable when identifying convergence or assigning adaptive function to morphological features, particularly those known only from fossil organisms.

Other differences between *X. audax* and *M. atlanticus* detected along PC1 were inconsistent between the 2D and 3D analysis. However, these sources of variation were relatively minor compared to those previously discussed, and may represent statistical artifacts or errors in the 3D reconstructions. One source of variation—the expanded buccal cavity along negative PC1—was only observable in the 3D analysis. This difference between the two species is likely an example of taphonomic bias. In life, it is likely that *X. audax* had a broader, rounded buccal cavity for accommodating prey, but the true curvature of the palatal and suspensorial bones of *X. audax* are unknown and were not speculated on for this study. Taphonomic flattening of these elements resulted in

reconstructions with buccal cavities that are more narrow and ‘triangular’ than they likely were in life. Despite this source of error not being present in the 2D analysis, both analyses still found nearly identical results, suggesting the difference in buccal width may not have been a major source of variation in the 3D analysis. However, if the proper proportions of the buccal cavity of *X. audax* were known and included in these reconstructions, it is likely the 3D between-species shape difference would have been reduced.

In addition to taphonomy, there were other potential sources of error in this study. While efforts were made to maintain consistent proportions in the arrangement of cranial elements between specimens (Fig. 1), human error remains a concern in any 3D reconstruction. However, the concordance of results between the 2D and 3D analyses does suggest that error introduced during 3D reconstruction was minimal relative to the shape difference between the two species. In analyses where morphological differences are more subtle, this type of human error may confound results more egregiously.

The exclusion of the supramaxillae from the analysis due to their tendency not to preserve in *X. audax* does have implications for the interpretation of differences in feeding. Based on known preserved specimens, the supramaxillae of *X. audax* differ in gestalt from that of *M. atlanticus*, being larger and more ovular compared to the smaller and more gracile supramaxillae of *M. atlanticus* (Gregory, 1933 pp. 139-141, 143; Bardack, 1965). The supramaxillae act as an insertion point for the *ligamentum maxilla-mandibulare anterius*, which connects the upper jaw to the mandible and assists in the opening and closing of the jaw (Vrba, 1968). Considering the large size of the

supramaxillae in *X. audax*, it can be speculated that *Xiphactinus* had particularly strong jaws for clamping down on prey. Because of the obvious differences in shape of the supramaxillae between these two species, the results presented here likely underestimate the differences between the feeding morphology of *X. audax* and *M. atlanticus*. Were the supramaxillae included, a greater degree of between-species separation reflecting vastly different feeding strategies is predicted. Finally, the particular selection of landmarks in this study are arbitrary—as they are in all landmark-based GM studies (Rohlf & Marcus, 1993)—and different landmark selection may produce different results. Landmarks in this study were selected to emphasize the feeding morphology by focusing on mandibular, maxillary, and suspensorial elements, with less emphasis placed on neurocranial elements or elements with unclear boundaries on specific specimens.

CONCLUSIONS

The purpose of this study is to quantify differences in the shape of the feeding morphology of the fish *Xiphactinus audax* and *Megalops atlanticus* to assess claims of structural convergence between the two species using landmark-based geometric morphometrics. Principle components analysis, SAHN clustering, and discriminant function analysis all show substantial differences in jaw shape between the two species. This is confirmed quantitatively by a multi-response permutation procedure, which shows that the species are significantly different in their shape ($p < 0.05$) and that there is high between-species differentiation and high within-group homogeneity. *X. audax* and *M. atlanticus* occupy discrete regions of morphospace with regard to their feeding structure, casting doubt on the claim that they are structurally convergent in this respect. Regardless, these results, alongside known feeding habits of these fish, indicate that *M. atlanticus* is a poor modern analog for *X. audax*.

Xiphactinus audax has a relatively large premaxilla strongly interdigitated with a relatively short maxilla, suggesting a jaw less well-adapted for suction feeding. Stomach contents of *X. audax* corroborate these results (Bardack, 1965), suggesting a much greater reliance on strong jaws and teeth to subdue large prey. By contrast, *M. atlanticus* has a much smaller, quadrangular premaxilla and a relatively longer maxilla, indicating a strong reliance on suction feeding. These results are, again, corroborated by known feeding habits of *M. atlanticus* as a predator of small, schooling fish (Grubich, 2001). Both species have deep mandibular symphyses, though their evolutionary history and different ecologies suggest this shared structure evolved to necessitate different functions.

Whereas *X. audax* likely evolved such a deep jaw to strengthen it against the forces of large thrashing prey, and to accommodate large teeth, *M. atlanticus* may have evolved this feature to increase buccal volume and improve suction feeding behavior. These results suggest structural convergence may occur even under different functional selective regimes.

At least one anatomical feature—the deep mandibular symphysis—appears to have undergone structural convergence between *X. audax* and *M. atlanticus*. This feature, however, likely evolved under different selective regimes and have not converged on a shared function. This conclusion is further supported by inferences regarding the feeding behavior of both species. Without knowledge of the last common ancestral form of *Xiphactinus* and *Megalops*, it is impossible to definitively state that no structural convergence has taken place between these species' feeding morphology, but the difference in their morphospace occupation does not support an interpretation of structural convergence. Additional research should incorporate ancestral state reconstruction, more diverse taxonomic sampling, and a larger sample size alongside comparative shape analysis to further examine the possibility and/or extent of structural convergence between *X. audax* and *M. atlanticus*, as well as other teleosts. This comparative anatomical work bears an organic fraternity with systematic studies. Including comparative anatomical work to substantiate claims of convergence in phylogenetic analysis may lead to more robust phylogenies—an area where potential convergence is a confounding factor (Arbuckle & Speed, 2016). Comparative GM analysis may also be useful in helping determine informative character states for

systematic analysis. This study was a granular look at a single study system, but there is much room for a higher resolution approach and a more robust understanding of convergence and the part it plays in the evolution of extinct organisms and their functional systems.

LITERATURE CITED

- Adams, D. C., and E. Otárola-Castillo. 2013. geomorph: an R package for the collection and analysis of geometric morphometric shape data. *Methods in Ecology and Evolution* 4:393-399.
- Adams, D. C., F. J. Rohlf, and D. E. Slice. 2004. Geometric morphometrics: ten years of progress following the 'revolution'. *Italian Journal of Zoology* 71:5-16.
- Adams, D. C. 2010. Parallel evolution of character displacement driven by competitive selection in terrestrial salamanders. *Evolutionary Biology* 10:72.
- Adams, A., K. Guindon, A. Horodysky, T. MacDonald, R. McBride, J. Shenker, and R. Ward. 2012. *Megalops atlanticus*. The IUCN Red List of Threatened Species 2012. Available at <http://dx.doi.org/10.2305/IUCN.UK.2012.RLTS.T191823A2006676.en>. Accessed June 5, 2019.
- Arbuckle, K., C. M. Bennett, and M. P. Speed. 2014. A simple measure of the strength of convergent evolution. *Methods in Ecology and Evolution* 5:685-693.
- Arbuckle, K., and M. P. Speed. 2016. Analysing Convergent Evolution: A Practical Guide to Methods; pp. 23-36 in P. Pontarotti (ed.) *Evolutionary Biology*. Springer International Publishing, Switzerland.
- Arratia, G., and H. Tischlinger. 2010. The first record of Late Jurassic crossognathiform fishes from Europe and their phylogenetic importance for teleostean phylogeny. *Fossil Record* 13:317-341.

- Bardack, D., and G. Sprinkle. 1969. Morphology and the relationship of saurocephalid fishes. *Fieldiana: Geology* 16:297-340.
- Bardack, D. 1965. Anatomy and evolution of chirocentrid fishes. *Vertebrata* 10:1-88.
- Beamon, J. C. 2001. Possible prey acquisition behavior for the Cretaceous fish *Xiphactinus audax*. *PaleoBios* 21:29.
- Cope, E. D. 1871a. Untitled letter. *Proceedings of the American Philosophical Society* 12:174-176.
- Cope, E. D. 1871b. On the Fossil Reptiles and Fishes of the Cretaceous Rocks of Kansas; pp. 385-424 in F. V. Hayden (ed.) *Fourth Annual Report of the United States Geological Survey of the Territories*. Government Printing Office, Washington, D.C.
- Cavender, T. 1966. The caudal skeleton of the Cretaceous teleost *Xiphactinus*, *Ichthyodectes*, and *Gillicus*, and its bearing in their relationship with *Chirocentrus*. *Occasional Papers on Zoology* 650:1-15.
- Cureton II, J. C., and R. E. Broughton. 2016. Rapid morphological divergence of a stream fish in response to changes in water flow. *Biology Letters* 10. Available at <http://dx.doi.org/10.1098/rsbl.2014.0352>. Accessed October 25, 2016.
- Dana, J. D., B. Silliman, A. Gray, W. Gibbs, H. A. Newton, S. W. Johnson, G. J. Brush, and A. E. Verrill. 1872. On Kansas vertebrate fossils. *American Journal of Science and Arts* 3:65.

- Deitloff, J., Cl. Floyd, and S. P. Graham. 2016. Examining head-shape differences and ecology in morphologically similar salamanders at their zone of contact. *Copeia* 104:233-242.
- Doolittle, R. F. 1994. Convergent evolution: the need to be explicit. *Trends in Biomedical Science* 19:15-18.
- Everhart, M. J., S. A. Hageman, and B. L. Hoffman. 2010. Another Sternberg “fish-within-a-fish” discovery: first report of *Ichthyodectes ctenodon* (Teleostei; Ichthyodectiformes) with stomach contents. *Transactions of the Kansas Academy of Science* 113:197-205.
- Filzmoser, P. 2018. Multivariate outlier detection based on robust methods. R package version 2.0.9. <https://cran.r-project.org/web/packages/mvoutlier/>.
- Gregory, W. K. 1933. Fish skulls: a study of the evolution of natural mechanisms. *Transactions of the American Philosophical Society* 23:75-481.
- Grubich, J. R. 2001. Prey capture in actinopterygian fishes: a review of suction feeding motor patterns with new evidence from an elopomorph fish, *Megalops atlanticus*. *American Zoologist* 41:1258-1265.
- Hay, O. P. 1898. Observations on the genus of fossil fishes called by Professor Cope, *Portheus*, by Dr. Leidy, *Xiphactinus*. *Zoological Bulletin* 2:25-54.
- Ingram, T., and L. Mahler. 2013. SURFACE: detecting convergent evolution from comparative data by fitting Ornstein-Uhlenbeck models with stepwise Akaike Information Criterion. *Methods in Ecology and Evolution* 4:416-425.

- Langerhans, R. B., C. A. Layman, A. K. Langerhans, and T. J. Dewitt. 2003. Habitat-associated morphological divergence in two Neotropical fish species. *Biological Journal of the Linnean Society* 80:689-698.
- Lauder, G. V., and Liem, K. F. 1983. The evolution and interrelationships of actinopterygian fishes. *Bulletin of the Museum of Comparative Zoology at Harvard College* 150:95-497.
- Leander, B. S. 2009. Different modes of convergent evolution reflect phylogenetic distances: a reply to Arendt and Reznick. *Trends in Ecology and Evolution* 23:481-482.
- Leander, B. S. 2008. A hierarchical view of convergent evolution in microbial eukaryotes. *Journal of Eukaryotic Microbiology* 55:59-68.
- Leidy, J. 1870. Remarks on the ichthyorudiolites and on certain fossil Mammalia. *Proceedings of the Academy of Natural Sciences of Philadelphia* 22:12-13.
- Leidy, J. 1873. Contributions to the Extinct Vertebrate Fauna of the Western Territories; in F. V. Hayden (ed.), *United States Geological Survey of the Territories, Volume 1*. Government Printing Office, Washington, D.C., 358 pp.
- Luther, G. 1985. Food and feeding habits of the two species of *Chirocentrus* from Mandapam. Ph. D. dissertation Central Marine Fisheries Research Institute, Waltair, India, 8 pp.
- Mahler, D. L., T. Ingram, L. J. Revell, and J. B. Losos. 2013. Exceptional convergence on the macroevolutionary landscape in island lizard radiations. *Science* 341:292-295.
- Maynrick, D., P. M. Brito, and O. Otero. 2015. Anatomical review of †*Salminops ibericus*, a Teleostei *incertae sedis* from the Cenomanian of Portugal, anciently assigned to

- Characiformes and possibly related to crossognathiform fishes. *Cretaceous Research* 56:66-75.
- McCune, B., and J. B. Grace (eds). 2002. *Analysis of Ecological Communities*. MJM Software Design, Gleneden Beach, Oregon, 300 pp.
- Moore, J., and P. Willmer. 1997. Convergent evolution in invertebrates. *Biological Reviews* 72:1-60.
- Müllner, D. 2011. Modern hierarchical, agglomerative clustering algorithms. ArXiv Technical Report.
- Murray, A. M., and T. D. Cook. 2016. Overview of the Late Cretaceous fishes of the northern Western Interior Seaway. *New Mexico Museum of Natural History Science Bulletin* 71:255-261.
- Muschick, M., A. Indermauer, and W. Salzburger. 2012. Convergent evolution within an adaptive radiation of cichlid fishes. *Current Biology* 22:2362-2368.
- Oksanen, J., F. G. Blanchet, M. Friendly, R. Kindt, P. Legendre, D. McGlinn, P. R. Minchin, R. B. O'Hara, G. L. Simpson, P. Solymos, M. H. H. Stevens, E. Szoecs, and H. Wagner. 2019. *Vegan: community ecology package*. R package version 2.4-6. <https://CRAN.R-project.org/package=vegan>.
- Osborn, H. F. 1904. The great Cretaceous fish *Portheus molossus* Cope. *Bulletin of the American Museum of Natural History* 20:377-381.

- Parsons, K. J., B. W. Robinson, and T. Hrbek. 2003. Getting into shape: an empirical comparison of the traditional truss-based morphometric methods with a newer geometric method applied to New World cichlids. *Environmental Biology of Fishes* 67:417-431.
- Piras, P., P. Colangelo, D. C. Adams, A. Buscalioni, J. Cubo, T. Kotsakis, C. Meloro, and P. Raia. 2010. The *Gavialis–Tomistoma* debate: the contribution of skull ontogenetic allometry and growth trajectories to the study of crocodylian relationships. *Evolution and Development* 12:568-579.
- Nelson, G. 1973. Notes on the structure and relationships of certain Cretaceous and Eocene teleostean fish. *American Museum Novitates* 2524:1-31.
- Paliy, O., and V. Shankar. 2016. Application of multivariate statistical techniques in microbial ecology. *Molecular Ecology* 25:1032-1057.
- Patterson, C., and D. E. Rosen. 1977. Review of ichthyodectiform and other Mesozoic teleost fishes and the theory and practice of classifying fossils. *Bulletin of the American Museum of Natural History* 158:83-172.
- R Core Team. 2017. R: a language and environment for statistical computing. R Foundation for Statistical Computing, Vienna, Austria. <https://www.R-project.org/>.
- Rohlf, F. J. 2019. tpsUtil. Stony Brook, NY: Department of Ecology and Evolution, State University of New York.
- Rohlf, F. J. 2010. tpsDig. Stony Brook, NY: Department of Ecology and Evolution, State University of New York.

- Rohlf, F. J., and L. F. Marcus. 1993. A revolution in morphometrics. *Trends in Ecology and Evolution* 8:139-132.
- Sakamoto, M., and M. Ruta. 2012. Convergence and divergence in the evolution of cat skulls: temporal and spatial patterns of morphological diversity. *PLoS ONE* 7. Available at [https:// doi:10.1371/journal.pone.0039752](https://doi:10.1371/journal.pone.0039752). Accessed October 15, 2017.
- Sokal, R. R., and F. J. Rohlf (eds.). 2009. *Introduction to Biostatistics*. Dover Publications, Mineola, New York, 363 pp.
- Schwimmer, D. R., J. D. Stewart, and G. D. Williams. 1997. *Xiphactinus vetus* and the distribution of *Xiphactinus* species in North America. *Journal of Vertebrate Paleontology* 17:310-615.
- Siwertsson, A., R. Knudsen, K. K. Kahilainen, K. Præbel, R. Primicerio, and P. Amundsen. 2010. Sympatric diversification as influenced by ecological opportunity and historical contingency in a young species lineage of whitefish. *Evolutionary and Ecology Research* 12:929-947.
- Skoglund, S., A. Siwertsson, P. Amundsen, and R. Knudsen. 2015. Morphological divergence between three Arctic charr morphs – the significance of the deep-water environment. *Ecology and evolution* 5:3114-3129.
- Slice, D. E. 2007. Geometric morphometrics. *Annual Review of Anthropology* 36:261-281.

- Souter, T., R. Cornette, J. Pedraza, J. Hutchinson, and M. Baylac. 2010. Two applications of 3D semi-landmark morphometrics implying different template designs: the theropod pelvis and the shrew skull. *Comptes Rendus Paleovol* 9:411-422.
- Speed, M. P., and K. Arbuckle. 2016. Quantification provides a conceptual basis for convergent evolution. *Biological Reviews* 92:815-829.
- Stayton, C. T. 2015. The definition, recognition, and interpretation of convergent evolution, and two new measures for quantifying and assessing the significance of convergence. *Evolution* 69:2140-2153.
- Stayton, C. T. 2006. Testing hypotheses of convergence with multivariate data: morphological and functional convergence among herbivorous lizards. *Evolution* 60:824-841.
- Stovall, J. W. 1933. *Xiphactinus audax*, a fish from the Cretaceous of Texas. University of Texas Bulletin 3201:87-92.
- Taverne, L. 2008. Considerations about the Late Cretaceous genus *Chirocentrites* and erection of the new genus *Heckelichthys* (Teleostei, Ichthyodectiformes) – a new visit inside the ichthyodectid phylogeny. *Bulletin de L'institut Royal des Sciences Naturelles de Belgique* 78:209-228.
- Valenciennes, M. A. 1846. Le Mégalope de l'Atlantique; pp. 398-401 in A. Paris and P. Bertrand (eds.), *Histoire Naturelle des Poissons*. Libraire de la Société Géologique de France, Strasbourg, France.

- Vavrek, M. J., A. M. Murray, and P. R. Bell. 2016. *Xiphactinus audax* Leidy 1870 from the Puskwaskau Formation (Santonian to Campanian) of north-western Alberta, Canada and the distribution of *Xiphactinus* in North America. *Vertebrate Anatomy Morphology Paleontology* 1:89-100.
- Venables, W. N., and B. D. Ripley (eds.). 2002. *Modern Applied Statistics with S* Fourth Edition. Springer Publishing, New York, New York, 498 pp.
- Vrba, E. S. 1968. Contributions to the functional morphology of fishes part V – the feeding mechanism of *Elops saurus* Linnaeus. *Zoologica Africana* 3:211-236.
- Wade, R. A. 1962. The biology of the tarpon *Megalops atlanticus*, and the ox-eye, *Megalops cyprinoides*, with emphasis on larval development. *Bulletin of Marine Science of the Gulf and Caribbean* 12:545-622.
- Walker, M. V. 2006. The impossible fish – revisited. *Transactions of the Kansas Academy of Science* 109:87-96.
- Westneat, M. W. 2005. Skull biomechanics and suction feeding in fishes. *Fish Biomechanics* 23:29-75.
- Westneat, M. W. 2004. Evolution of levers and linkages in the feeding mechanisms of fish. *Integrative Comparative Biology* 44:378-389.
- Whitehead, P. J. P., and R. Vergara. 1978. Megalopidae; in W. Fischer, G. Bianchi, and W. B. Scott (eds.), *FAO species identification sheets for fishery purposes Western Central Atlantic (Fishing Area 31), Volume 2*. Department of Fisheries and Oceans, Ottawa, 4 pp.

- Wiley DF, Amenta N, Alcantara DA, Ghosh D, Kil YJ, Delson E, Harcourt-Smith W, Rohlf FJ, St John K, Hamann B. 2005. Evolutionary morphing. *Proc IEEE Vis 2005* 431–438.
- Wray, G. A. 2002. Do convergent developmental mechanisms underlie convergent phenotypes? *Brain, Behavior, and Evolution* 59:327-336.
- Zelditch, M. L., D. L. Swiderski, and H. D. Sheets (eds.). 2012. *Geometric Morphometrics for Biologists: a Primer*. Academic Press, San Diego, California, 478 pp.
- Zimmerman, G. M., H. Goetz, and P. W. Mielke Jr. 1985. Use of an improved statistical method for group comparisons to study effects of prairie fire. *Ecology* 66:606-611.

TABLES AND FIGURES

Table 1. Study specimens and their standard length in descending order of size (* denotes standard length estimated from cranial material; red text indicates specimens removed as outliers).

Catalog Number	Taxon	State of Articulation	Standard Length (cm)
AMNH FF-1951	<i>X. audax</i>	partially articulated cranium	413*
FHSM VP-333	<i>X. audax</i>	fully articulated	407.4
FHSM VP-699	<i>X. audax</i>	articulated cranium	336*
USNM V-11653	<i>X. audax</i>	articulated cranium	322*
YPM VP-56875	<i>X. audax</i>	articulated cranium	311*
USNM V-11554	<i>X. audax</i>	articulated cranium	301*
USNM 260337	<i>M. atlanticus</i>	partially articulated cranium	268*
TNHC 62473	<i>M. atlanticus</i>	disarticulated	219.1
NCSM 45757	<i>M. atlanticus</i>	disarticulated	215.9
AMNH 211548-SD	<i>M. atlanticus</i>	partially articulated cranium	197*
USNM 21554	<i>M. atlanticus</i>	partially articulated cranium	177*
UF 10674-S	<i>M. atlanticus</i>	disarticulated	156*

Table 2. MRPP analysis values (* denotes significant p-value < 0.05).

Treatment	p-value	A	T
2D unadjusted	0.002*	0.774	-7.34
2D outlier-adjusted	0.006*	0.856	-5.76
3D unadjusted	0.002*	0.758	-7.34
3D outlier-adjusted	0.005*	0.823	-5.86

Table 3. Explanatory values of the first four PC axes for each treatment.

		PC 1	PC 2	PC 3	PC 4
2D unadjusted	Proportion of Variance	0.68178	0.10988	0.0683	0.05668
	Cumulative Proportion	0.68178	0.79166	0.85996	0.91664
	Eigenvalue	8.18136	1.31856	0.8196	0.68016
3D unadjusted	Proportion of Variance	0.66057	0.12069	0.06935	0.05981
	Cumulative Proportion	0.66057	0.78126	0.85062	0.91042
	Eigenvalue	7.92684	1.44828	0.8322	0.71772
2D outlier-adjusted	Proportion of Variance	0.73407	0.0972	0.06095	0.03596
	Cumulative Proportion	0.73407	0.83128	0.89223	0.92819
	Eigenvalue	7.3407	0.972	0.6095	0.3596
3D outlier-adjusted	Proportion of Variance	0.70932	0.10474	0.06859	0.03951
	Cumulative Proportion	0.70932	0.81407	0.88266	0.92217
	Eigenvalue	7.0932	1.0474	0.6859	0.3951

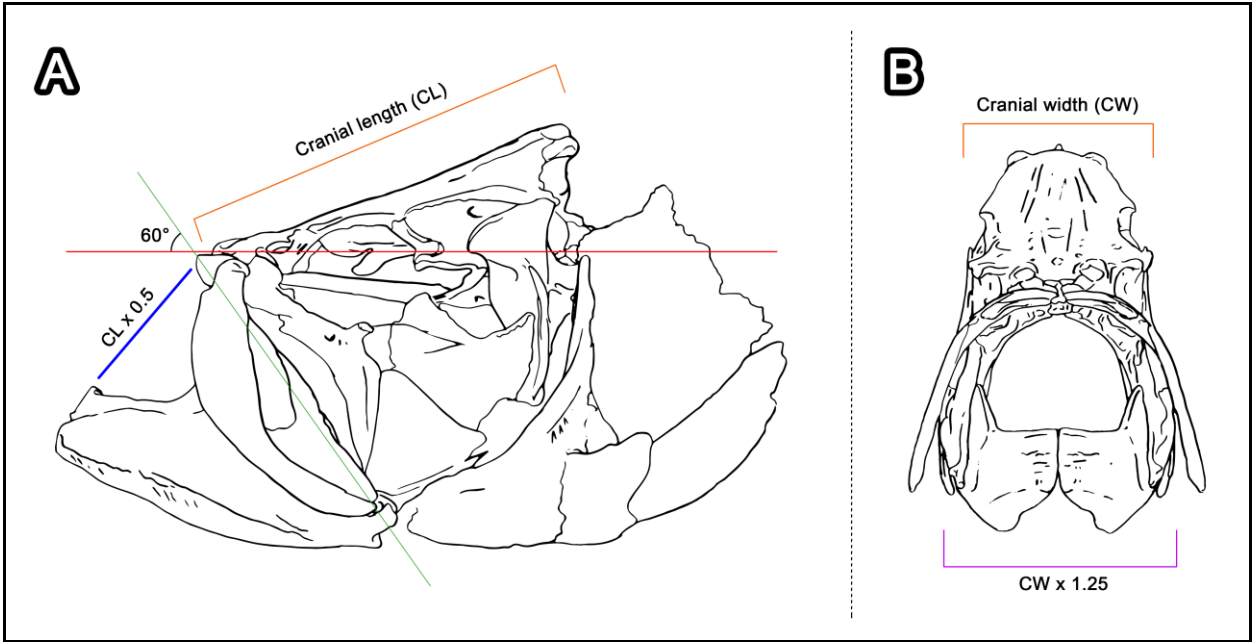


Figure 1. Interpretive line drawings of NCSM 45757 showing measurements for jaw angle and gape size in left lateral aspect (A), and gape width in anterior aspect (B). Jaw angle (green) is set to 60° from the axis of the occipital condyle (red). Gape size (blue) is set to 0.5 times the cranial length (CL). Gape width (purple) is set to 1.25 times the cranial width (CW).

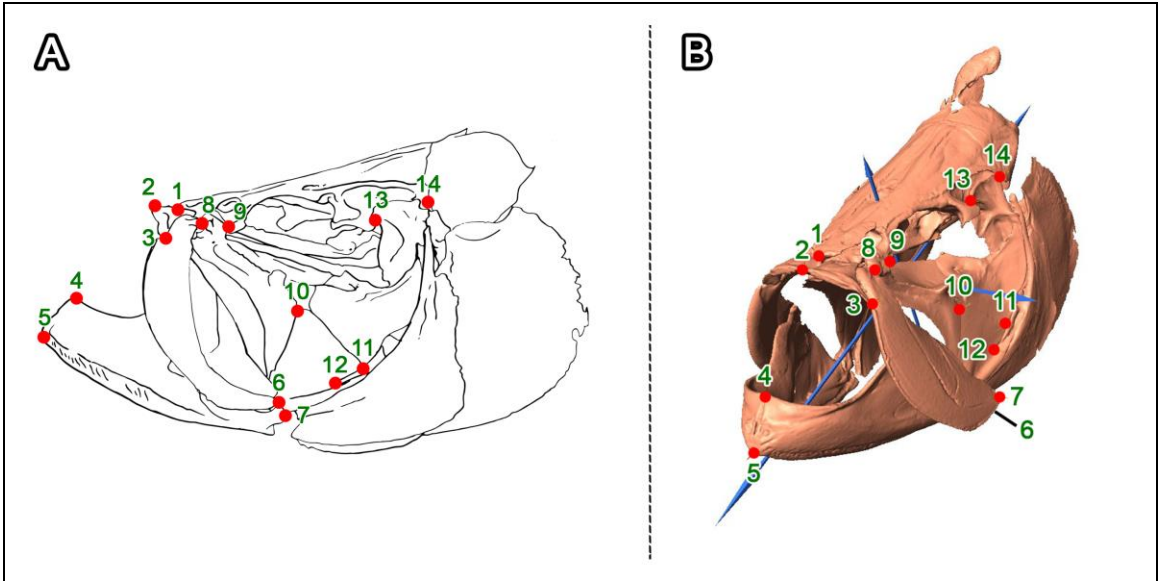


Figure 2. Example of landmark placement on 2D interpretive line drawing (A) and 3D model (B) of AMNH 21154. 2D analysis used 14 landmarks and 3D analysis used 24 landmarks (14 visible).

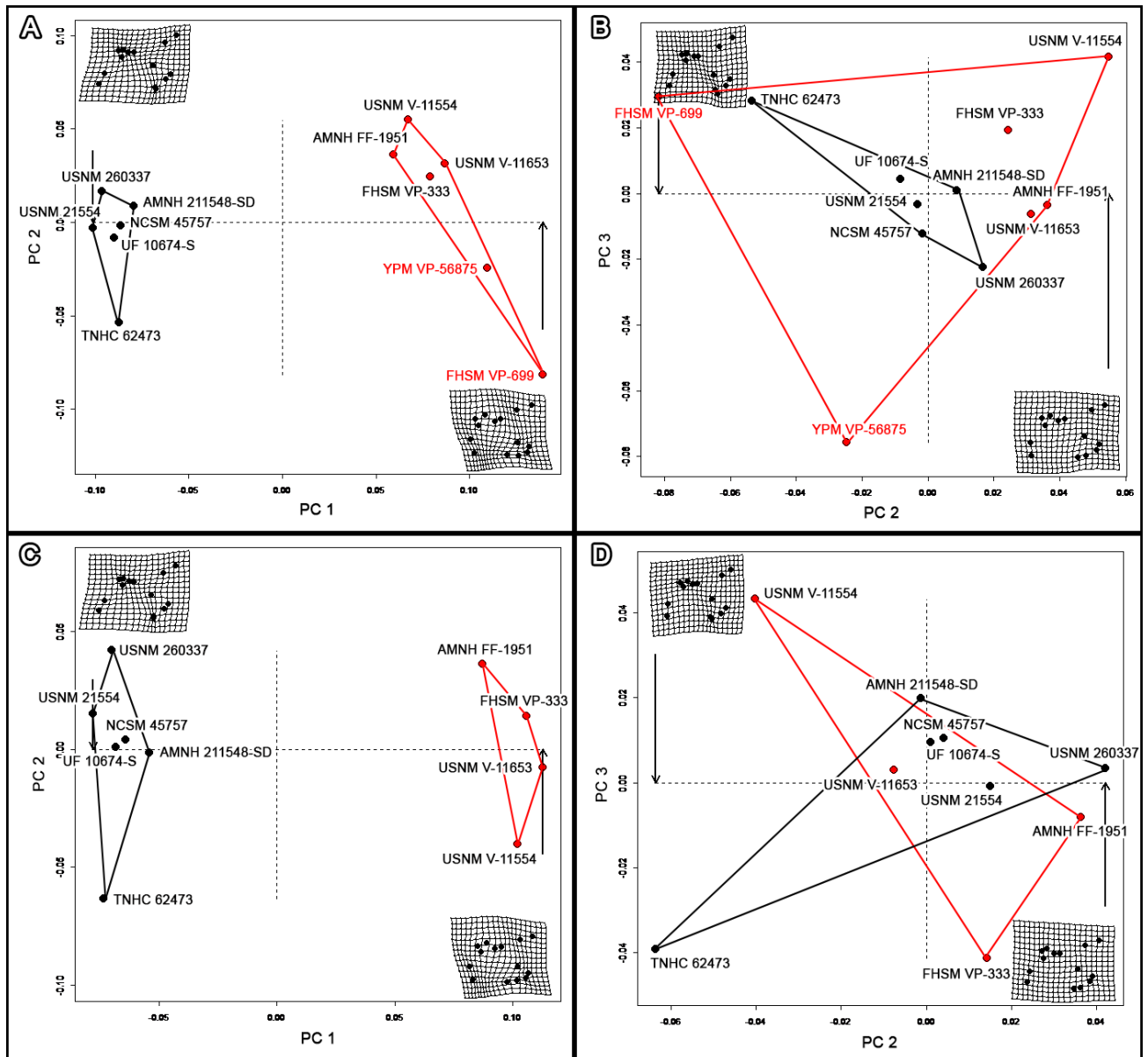


Figure 3. PC morphospace for all 2D treatments. Black dots and polygons indicate *M. atlanticus* specimens. Red dots and polygons indicate *X. audax* specimens. Red text indicates outlier specimens. Deformation grids indicate shape change along negative (upper left) and positive (bottom right) PC X-axis. (A) 2D unadjusted analysis PC1 and PC2: PC1 explains 68.2% of the variation; PC2 explains 11.0% of the variation (B) 2D unadjusted analysis PC2 and PC3: PC2 explains 11.0% of the variation; PC3 explains 6.9% of the variation (C) 2D outlier-adjusted analysis PC1 and PC2: PC1 explains 73.0% of the variation; PC2 explains 9.7% of the variation (D) 2D outlier-adjusted analysis PC2 and PC3: PC2 explains 9.7% of the variation; PC3 explains 6.1% of the variation.

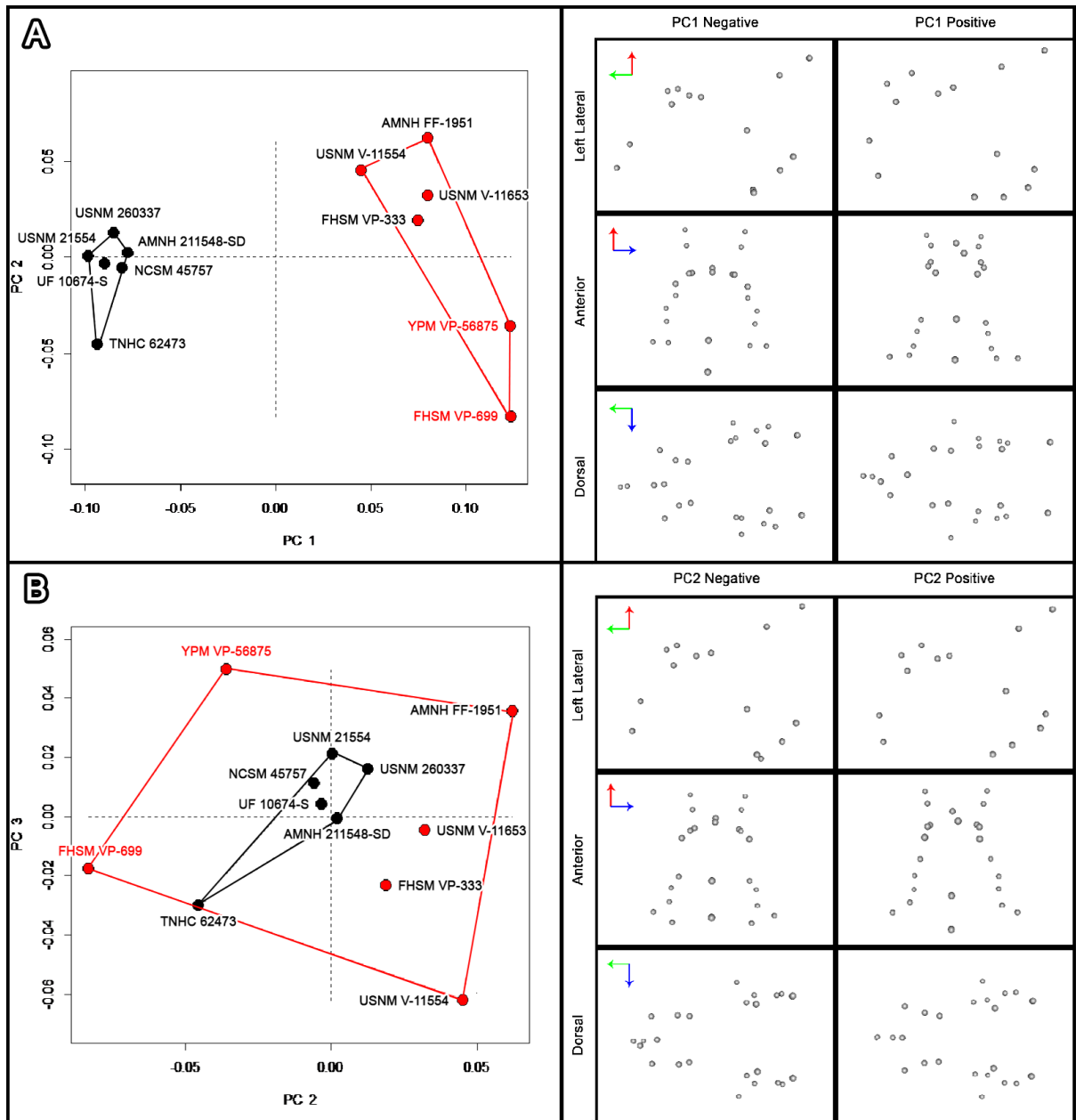


Figure 4. PC morphospace for the unadjusted 3D treatment. Black dots and polygons indicate *M. atlanticus* specimens. Red dots and polygons indicate *X. audax* specimens. Red text indicates outlier specimens. Point clouds representing landmarks show the source of shape variation along the PC X-axis in left lateral (top), anterior (middle), and dorsal (bottom) aspects. Shape variation described by negative PC values is shown in the left column. Shape variation described by positive PC values is shown in the right column. Red arrows point dorsally, green arrows point anteriorly, and blue arrows point towards left lateral aspect. (A) PC1 and PC2: PC1 explains 66.1% of the variation; PC2 explains 12.1% of the variation (B) PC2 and PC3: PC2 explains 12.1% of the variation; PC3 explains 6.9% of the variation

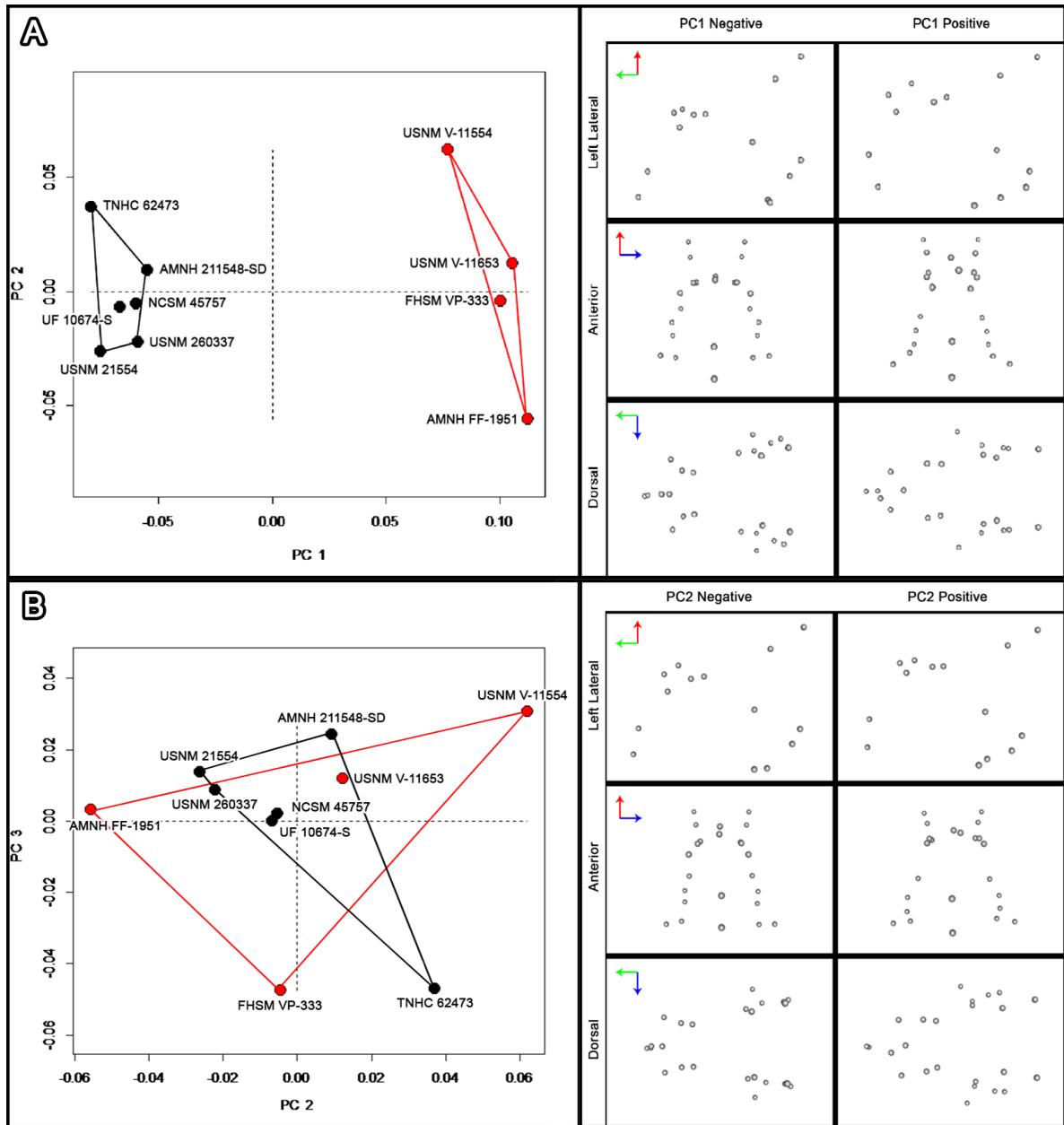


Figure 5. PC morphospace for the outlier-adjusted 3D treatment. Black dots and polygons indicate *M. atlanticus* specimens. Red dots and polygons indicate *X. audax* specimens. Red text indicates outlier specimens. Point clouds representing landmarks show the source of shape variation along the PC X-axis in left lateral (top), anterior (middle), and dorsal (bottom) aspects. Shape variation described by negative PC values is shown in the left column. Shape variation described by positive PC values is shown in the right column. Red arrows point dorsally, green arrows point anteriorly, and blue arrows point towards left lateral aspect. (A) PC1 and PC2: PC1 explains 71.0% of the variation; PC2 explains 10.5% of the variation (B) PC2 and PC3: PC2 explains 10.5% of the variation; PC3 explains 6.9% of the variation.

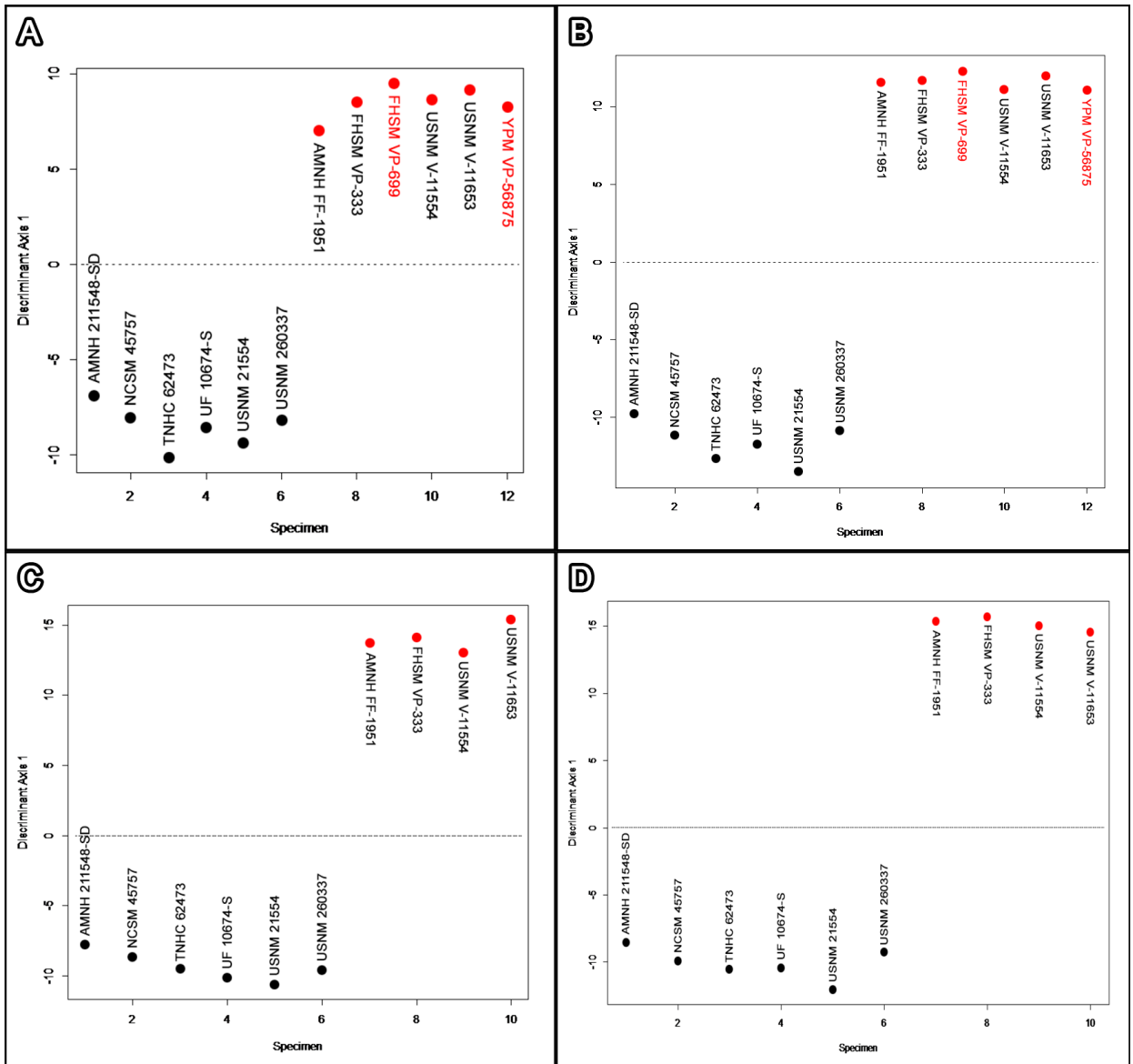


Figure 6. DFA plot showing specimen groupings for 2D unadjusted (A), 3D unadjusted (B), 2D outlier adjusted (C), and 3D outlier-adjusted (D) treatments along LD1 (Y-axis). Black dots represent *M. atlanticus* specimens and red dots indicate *X. audax* specimens. Red text indicates outlier specimens.

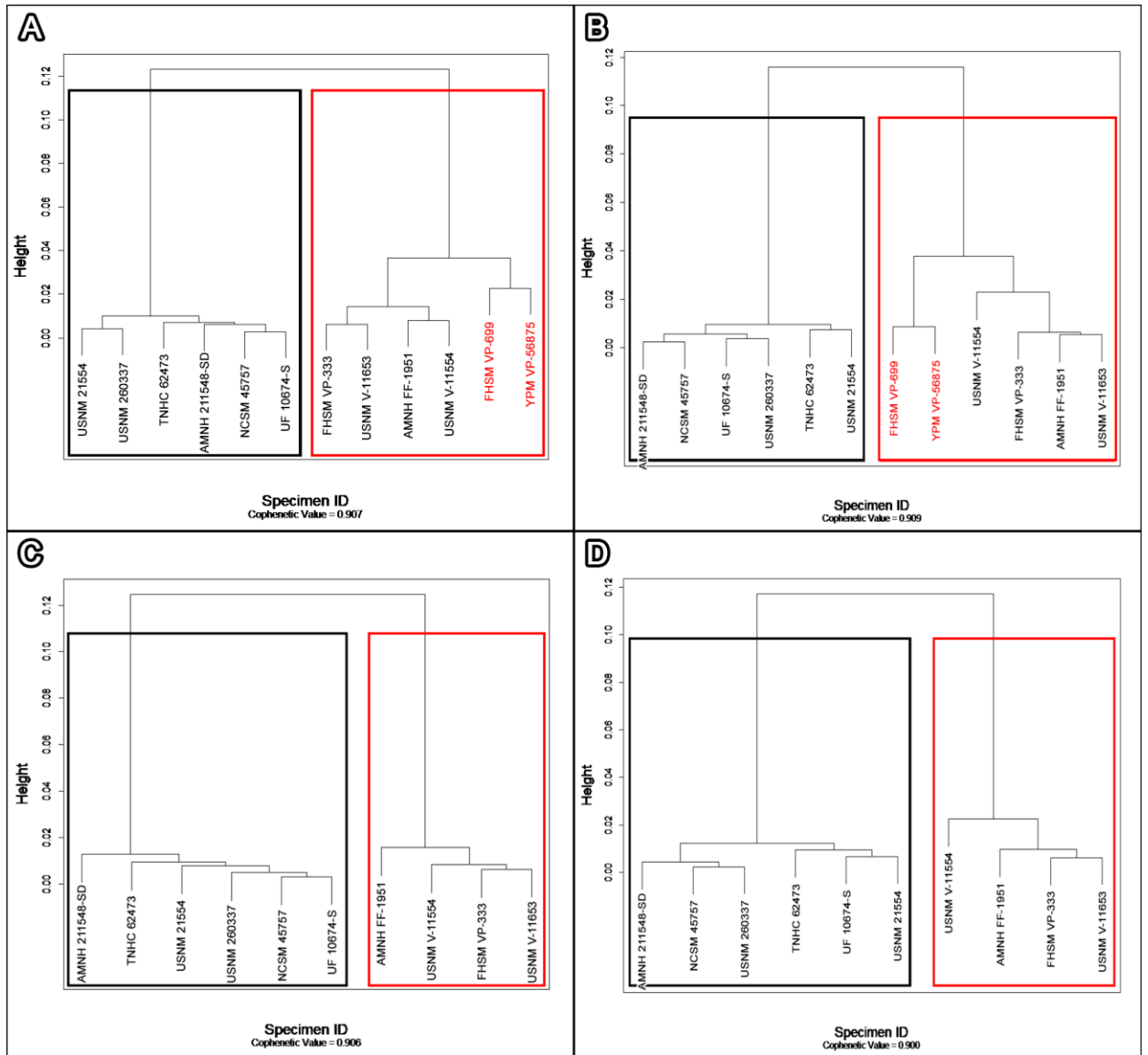


Figure 7. SAHN cluster dendrograms for all 2D and 3D treatments. Black boxes indicate *M. atlanticus* specimens. Red boxes indicate *X. audax* specimens. (A) 2D unadjusted: cophenetic value = 0.907 (B) 3D unadjusted: cophenetic value = 0.909 (C) 2D outlier-adjusted: cophenetic value = 0.906 (D) 3D outlier-adjusted: cophenetic value = 0.900.

**Fort Hays State University
FHSU Scholars Repository
Non-Exclusive License Author Agreement**

I hereby grant Fort Hays State University an irrevocable, non-exclusive, perpetual license to include my thesis ("the Thesis") in *FHSU Scholars Repository*, FHSU's institutional repository ("the Repository").

I hold the copyright to this document and agree to permit this document to be posted in the Repository, and made available to the public in any format in perpetuity.

I warrant that the posting of the Thesis does not infringe any copyright, nor violate any proprietary rights, nor contains any libelous matter, nor invade the privacy of any person or third party, nor otherwise violate FHSU Scholars Repository policies.

I agree that Fort Hays State University may translate the Thesis to any medium or format for the purpose of preservation and access. In addition, I agree that Fort Hays State University may keep more than one copy of the Thesis for purposes of security, back-up, and preservation.

I agree that authorized readers of the Thesis have the right to use the Thesis for non-commercial, academic purposes, as defined by the "fair use" doctrine of U.S. copyright law, so long as all attributions and copyright statements are retained.

To the fullest extent permitted by law, both during and after the term of this Agreement, I agree to indemnify, defend, and hold harmless Fort Hays State University and its directors, officers, faculty, employees, affiliates, and agents, past or present, against all losses, claims, demands, actions, causes of action, suits, liabilities, damages, expenses, fees and costs (including but not limited to reasonable attorney's fees) arising out of or relating to any actual or alleged misrepresentation or breach of any warranty contained in this Agreement, or any infringement of the Thesis on any third party's patent, trademark, copyright or trade secret.

I understand that once deposited in the Repository, the Thesis may not be removed.

Thesis: An Assessment of Convergence in the Feeding Morphology of *Xiphactinus audax* and *Megalops atlanticus* using Landmark-Based Geometric Morphometrics

Author: Edward Chase Holt Shelburne

Signature: 

Date: 27 Apr 2020